Potential recycling of thaumarchaeotal lipids by DPANN Archaea in seasonally hypoxic surface marine sediments

Yvonne A. Lipsewers[a], Ellen C. Hopmans[a], Jaap S. Sinninghe Damsté[a,b], Laura Villanueva[a*]

[a] *NIOZ Royal Netherlands Institute for Sea Research, Department of Marine Microbiology and Biogeochemistry, and Utrecht University, P.O. Box 59, 1797AB Den Burg, Texel, The Netherlands*

[b] *Faculty of Geosciences. Department of Earth Sciences, Utrecht University., P.O. Box 80.021, 3508 TA Utrecht, The Netherlands*

Keywords: Thaumarchaeota, crenarchaeol, glycerol dibiphytanyl glycerol tetraether (GDGT), DPANN, Woesearchaeota, hypoxia, marine sediments.

Running title: DPANN Archaea potentially recycle thaumarchaeotal lipids

[*]Corresponding author. *E mail*: laura.villanueva@nioz.nl (Laura Villanueva).

ABSTRACT

Thaumarchaeota synthesize specific glycerol dibiphytanyl glycerol tetraethers (GDGTs), the distribution of which is affected by temperature, thereby forming the basis of the paleotemperature proxy TEX_{86}. Lipids in marine surface sediments are believed to be derived mainly from pelagic Thaumarchaeota; however, some studies have evaluated the possibility that benthic Archaea also contribute to the lipid fossil record. Here, we compared the archaeal abundance and composition from DNA-based methods and the archaeal intact polar lipid (IPL) diversity in surface sediments of a seasonally hypoxic marine lake to determine the potential biological sources of the sedimentary archaeal IPLs in under changing environmental conditions. The archaeal community changed from March (oxic conditions) to August (euxinic) from a Thaumarchaeota-dominated community (up to 82%) to an archaeal community dominated by the DPANN super phylum (up to 95%). This marked change coincided with a one order of magnitude decrease in the total IPL-GDGT abundance. In addition, IPL-GDGTs with glyco-polar head group increased. This may indicate a transition to Thaumarchaeota growing in stationary phase or selective preservation of the GDGT pool. In addition, considering the apparent inability of the DPANN Archaea to synthesize their own membrane lipids, we hypothesize that the dominant DPANN Archaea population present in August use the lipids synthesized previously by the Thaumarchaeota or other Archaea to form their own cell membranes, which would indicate an active recycling of fossil IPLs in the marine surface sediment.

1. Introduction

Archaea occur ubiquitously, are abundant in aquatic and terrestrial habitats and play an important role in global biogeochemical cycles (Jarrell et al., 2011). Marine sediments have been shown to harbor a diverse archaeal community, including ammonia-oxidizing Thaumarchaeota (marine group I.1a) (Pester et al., 2011), as well as Bathyarchaeota formerly known as Miscellaneous Crenarchaeota Group (MCG), Marine Benthic Group-B (MBG-B) and MBG-D, and Archaea of the DPANN (Diapherotrites, Parvarchaeota, Aenigmarchaeota, Nanoarchaeota and Nanohaloarchaeota) super phylum, of which the latter are predicted to be involved in degradation of polymers and proteins under anoxic conditions (Lloyd et al., 2013, Meng et al., 2014; Castelle et al., 2015).

Archaeal lipids are widespread in marine sediments and are commonly used as biomarkers of Archaea both in present-day systems and in past depositional environments. However, their biological sources are not well constrained, especially in the light of the expanding archaeal diversity. Archaeal lipids in marine surface sediments are thought to be derived mainly from pelagic Thaumarchaeota which, due to grazing and packing in fecal pellets, are efficiently transported to the sediment where they become preserved in the sedimentary record (Huguet et al., 2006a). Thaumarchaeota synthesize isoprenoid glycerol dibiphytanyl glycerol tetraethers (GDGTs) containing 0–4 cyclopentane moieties (GDGT-0 to GDGT-4) as well as the GDGT crenarchaeol (Sinninghe Damsté et al., 2002), containing 4 cyclopentane moieties and a cyclohexane moiety, which is considered to be characteristic of this phylum (Pearson et al., 2004; Zhang et al., 2006; Pester et al., 2011; Pitcher et al., 2011a; Sinninghe Damsté et al., 2012). The distribution of thaumarchaeotal GDGTs in the marine environment is affected by temperature, i.e. with increasing temperature there is an increase in the relative abundance of cyclopentane-

containing GDGTs (Schouten et al., 2002; Wuchter et al., 2004, 2005). Based on this relationship, the TEX_{86} paleotemperature proxy was developed and calibrated vs. sea surface temperature (e.g. Schouten et al., 2002; Kim et al., 2010) and has been widely applied for more than a decade (Schouten et al., 2013).

Although it is generally thought that GDGTs in marine sediments derive from surface-derived thaumarchaeotal biomass (e.g. Wakeham et al., 2003), some studies have addressed the possibility of a potential contribution of lipids of benthic Archaea to the fossil record, which would be relevant for the reliability of TEX_{86} (Biddle et al., 2006; Shah et al., 2008; Lipp et al., 2008; Lipp and Hinrichs, 2009). Archaeal intact polar lipids (IPLs), where the core lipid (CL) GDGTs are attached to polar head groups from the building blocks of membranes of living cells with phospho- head groups have been shown to degrade rapidly upon death of the source organism (White et al., 1979; Harvey et al., 1986), while IPLs with glyco- polar head groups may be preserved over (much) longer timescales (Longemann et al., 2010; Bauersachs et al., 2010; Xie et al., 2013). IPLs of Archaea have been detected in surface marine sediments and used as biomarkers of the presence of benthic Archaea living in situ (Biddle et al., 2006; Lipp et al., 2008; Lipp and Hinrichs, 2009; Lengger et al., 2012). In addition, some studies have suggested that benthic marine Archaea recycle fossil CL-GDGTs when producing IPL-GDGTs de novo to decrease energy requirements (Liu et al., 2011; Takano et al., 2010).

With the exception of Thaumarchaeota, the membrane lipid composition of other phyla of benthic Archaea present in marine sediments has not been characterized, so their potential impact on the archaeal lipid pool preserved in the sedimentary record remains unknown. In surface sediments where O_2 is still available, Thaumarchaeota are expected to be dominant due to their oxygenic metabolism as nitrifiers (Könneke et al., 2005, Wuchter et al., 2006). However, in subsurface sediments, where O_2 is no longer present, archaeal groups such as MBG-D, MCG,

Thermoplasmatales and methanogens have been reported to be predominant (Kubo et al., 2012; Lloyd et al., 2013), and may contribute to the total archaeal lipid pool in marine sediments. Recent studies have also observed a significant presence of Archaea of the super phylum DPANN, both in surface and subsurface coastal marine sediments (Choi et al., 2016), as well as in freshwater systems (Ortiz-Alvarez et al., 2016; Ma et al., 2016). However, their contribution to the sedimentary archaeal lipid pool is expected to be negligible as their small genomes (Castelle et al., 2015) lack the genes of the membrane lipid biosynthetic pathway, suggesting that they rely on host cells or cell debris for the synthesis of their lipids (Waters et al., 2003; Jahn et al., 2004).

Here, we have determined the archaeal abundance and composition, using DNA-based methods, in surface sediments of a seasonally hypoxic marine lake with different O_2 and S^{2-} bottom water concentrations and compared them with the composition of the archaeal IPLs. The aim was to identify the potential biological sources of the archaeal IPL lipids detected in surface sediments under changing environmental conditions, which could impact the biology of the producer but also the preservation potential of the archaeal lipids.

2. Material and methods

2.1. Study site, sediment sampling and physicochemical analysis

Lake Grevelingen is a former estuary within the Rhine-Meuse-Scheldt delta area of the Netherlands. The delta became a closed saline reservoir (salinity ca. 30) by way of dam construction at both the land side and sea side in the early 1970s. As a result of the absence of tides and strong currents, the lake experiences seasonal stratification of the water column which, in turn, leads to a depletion of O_2 in the bottom water (Hagens et al., 2015). Bottom water O concentration at the deepest stations starts to decline in April, reaches hypoxic conditions by end

111 of May (O_2 < 63 µM), and further decreases to reach the state of anoxia in August (O_2 <0.1 µM),
112 with re-oxygenation of the bottom water taking place in September (Seitaj et al., 2015).
113 Two sampling campaigns were performed on March 13th, 2012 (before the start of the annual
114 O_2 depletion) and on August 20th, 2012 (at the peak of the annual O_2 depletion). Detailed water
115 column, porewater and solid sediment chemistry of the lake over the year 2012 have been
116 reported (Seitaj et al., 2015; Hagens et al., 2015; Sulu-Gambari et al., 2016). Intact sediment
117 cores were recovered at three stations along a depth gradient within the Den Osse basin, one of
118 the deeper basins in this marine lake: Station 1 (S1) was at the deepest point (34 m) of the basin
119 (51.747°N, 3.890°E), Station 2 (S2) at 23 m (51.749°N, 3.897°E) and Station 3 (S3) at 17 m
120 (51.747°N, 3.898°E) (Fig. 1). Cores were retrieved with a single core gravity corer (UWITEC)
121 using PVC core liners (60 cm × 6 cm i.d.). Further details of the sampling have been described in
122 detail by Lipsewers et al. (2017). Four cores were sliced at 1 cm resolution (for the purposes of
123 this study we focused only on the top 1 cm) for lipid and DNA/RNA analysis and kept at –80 ºC
124 until further processing.
125 Total organic carbon (TOC) content was determined on sub-samples that were freeze-dried,
126 ground to a fine powder and analyzed using isotope ratio monitoring mass spectrometry (irm MS;
127 Thermo Finnigan Delta plus) with connected to a Flash 2000 elemental analyzer (Thermo Fisher
128 Scientific, Milan). Before analysis, samples were acidified with 2N HCl to remove inorganic
129 carbon (Nieuwenhuize et al., 1994). Concentration of TOC is expressed as mass % of dry
130 sediment. O_2, S^{2-}, bottom water and porewater NH_4^+, NO_2^- and NO_3^- were determined as
131 previously described (Malkin et al., 2014; Seitaj et al., 2015) and reported by Lipsewers et al.
132 (2017).
133 *2.2. DNA/RNA extraction*

Each sediment sample (0-1 cm) was centrifuged and excess H_2O removed by pipetting before extraction of nucleic acids from the sediment. DNA/RNA was extracted with the RNA PowerSoil® Total Isolation Kit plus the DNA elution accessory (Mo Bio Laboratories, Carlsbad, CA). Concentration of DNA was quantified by Nanodrop (Thermo Scientific, Waltham, MA, USA) and Fluorometric with Quant-iT^{TM} PicoGreen® dsDNA Assay Kit (Life Technologies, The Netherlands).

2.3. 16S rRNA gene amplicon sequencing and sequencing analysis

PCR reactions were performed with the universal Bacteria and Archaea primers S-D-Arch-0159-a-S-15 and S-D-Bact-785-a-A-21 (Klindworth et al., 2013) as described by Moore et al. (2015). The archaeal 16S rRNA gene amplicon sequences were analyzed with QIIME v1.9 (Caporaso et al., 2010). Raw sequences were demultiplexed and quality-filtered with a minimum quality score of 25, length between 250 and 350, and allowing a maximum two errors in the barcode sequence. Taxonomy was assigned based on blast and the SILVA database version 123 (Altschul et al., 1990; Quast et al., 2013). The 16S rRNA gene amplicon reads (raw data) have been deposited in the NCBI Sequence Read Archive (SRA) under BioProject no. PRJNA293286.

2.4. PCR amplification, cloning and archaeal 16S rRNA gene quantification

Amplification of the archaeal *amoA* gene was performed as described by Yakimov et al. (2011). The PCR reaction mixture was the following (final concentration): Q-solution 1× (PCR additive, Qiagen); PCR buffer 1×; Bovine Serum albumin (BSA) (200 mM); Deoxynucleotide (dNTP) Solution Mix (20 µM); primers (0.2 µM); $MgCl_2$ (1.5 mM); 1.25 U Taq polymerase (Qiagen, Valencia, CA, USA). PCR conditions were: 95 °C, 5 min; 35 × [95 °C, 1 min; 55 °C, 1 min; 72 °C, 1 min]; final extension 72 °C, 5 min. PCR products were gel purified (QIAquick gel purification kit, Qiagen) and cloned in the TOPO-TA cloning® kit from Invitrogen (Carlsbad,

157 CA, USA) and transformed in *Escherichia coli* TOP10 cells following the manufacturer's
158 recommendations. Recombinant clones plasmid DNA were purified by Qiagen Miniprep kit and
159 screening by sequencing ($n \geq 30$) using M13R primer by BaseClear (Leiden, The Netherlands).
160 Resulting archaeal *amoA* protein sequences were aligned with already annotated *amoA* sequences
161 by using the Muscle application (Edgar, 2004). Phylogenetic trees were constructed with the
162 Neighbor-Joining method (Saitou and Nei, 1987) and evolutionary distances computed using the
163 Poisson correction method with a bootstrap test of 1,000 replicates.
164 Quantification of archaeal 16S rRNA gene copies was performed by quantitative PCR (qPCR),
165 using the primers Parch519F and ARC915R as described by Pitcher et al. (2011b).
166 *2.5. Lipid extraction and analysis*
167 Total lipids were extracted after freeze-drying using a modified Bligh and Dyer method (Bligh
168 and Dyer, 1959) following a protocol described by Lengger et al. (2014). Each extract was then
169 dissolved by adding hexane:isopropanol:H_2O, 718:271:10 (v/v/v) and filtering through a 0.45
170 µm, 4 mm diameter true regenerated cellulose syringe filter (Grace Davison, Columbia, MD,
171 USA).
172 IPLs were analyzed using ultra high pressure liquid chromatography-high resolution mass
173 spectrometry (UHPLC-HR MS). An Ultimate 3000 RS UHPLC, equipped with thermostated
174 auto-injector and column oven, coupled to a Q Exactive Orbitrap MS with Ion Max source with
175 heated electrospray ionization (HESI) probe (Thermo Fisher Scientific, Waltham, MA), was
176 used. UHPLC conditions were: thermostatted auto-injector and column oven, YMC-Triart Diol-
177 HILIC column (250 x 2.0 mm, 1.9 µm particles, pore size 12 nm; YMC Co., Ltd, Kyoto, Japan)
178 at 30 °C . The elution program at 0.2 ml/min was: 100% A (5 min), followed by a linear gradient
179 to 66% A:34% B in 20 min (held 15 min), followed by a linear gradient to 40% A:60% B in 15
180 min, followed by a linear gradient to 30% A:70% B in 10 min, where A = hexane/2-

propanol/formic acid/14.8 M NH_3 aq (79:20:0.12:0.04; v/v/v/v) and B = 2-propanol/water/formic acid/14.8 M NH_3 aq. (88:10:0.12:0.04; v/v/v/v). Total run time was 70 min, with re-equilibration 20 min between runs. HR MS (Q Exactive Orbitrap, Ion Max source, heated electrospray ionization [HESI] probe; Thermo Fisher Scientific, Waltham, MA) used the following HESI settings: sheath gas (N_2) pressure 35 (arbitrary units), auxiliary gas (N_2) pressure 10 (arbitrary units), auxiliary gas (N_2) T 50 ˚C, sweep gas (N_2) pressure 10 (arbitrary units), spray voltage 4.0 kV (positive ion ESI), capillary 275 °C, S-Lens 70 V. IPLs were analyzed with a range of *m/z* 375 to 2000 (resolution 70,000), followed by data-dependent MS^2 (resolution 17,500), in which the 10 most abundant masses in the spectrum (with the exclusion of isotope peaks) were fragmented successively (stepped normalized collision energy 15, 22.5, 30; isolation window 1.0 *m/z*). An inclusion list was used with a mass tolerance of 3 ppm to target specific compounds (supplementary File A.1). The MS instrument was calibrated within a mass accuracy range of 1 ppm using the Thermo Scientific Pierce LTQ Velos ESI Positive Ion Calibration Solution (containing a mixture of caffeine, MRFA, Ultramark 1621 and *n*-butylamine in acetonitrile/methanol/acetic acid solution). IPLs were quantified by integrating the summed mass chromatograms (within 3 ppm accuracy) of the dominant adduct formed (in the case of monohexose, MH-, dihexose, DH- and hexose phosphohexose, HPH-IPLs the ammoniated adduct) and the first isotopomer and reported as peak area response/g dry sediment extracted, due to the lack of quantitative standards (for details see Pitcher et al., 2011b).

The total lipid extract was further analyzed by way of acid hydrolysis to determine the composition and relative abundance of IPL-derived CLs (resulting from the hydrolysis of IPLs) and CL-GDGTs using the method described by Lengger et al. (2012) and analyzed via HPLC-atmospheric pressure chemical ionization MS (HPLC-APCI MS; Schouten et al., 2007) using an internal C_{46} GDGT standard as described by Huguet al. (2006b).

205 # 3. Results

206 *3.1. Physicochemical conditions*

207 The seasonal variation in the bottom water O_2 concentration in the lake strongly influenced the
208 bottom water and porewater concentration of O_2 and S^{2-} (Table 1). In March, the bottom water
209 was fully oxygenated at all stations (299–307 μM), O_2 penetrated to 1.8–2.6 mm in the sediment
210 and no free S^{2-} was recorded in the first few cm (Hagens et al., 2015). The width of the suboxic
211 zone, operationally defined as the sediment layer between the O_2 penetration depth (OPD) and
212 the S^{2-} appearance depth (SAD), varied between 16 and 39 mm across the three stations in March
213 2012. In contrast, in August, O_2 was strongly depleted in the bottom water at S1 (< 0.1 μM) and
214 S2 (11 μM) and no O_2 was detected from microsensor profiling in the surface sediment at these
215 two stations. At S3, the bottom water concentration of O_2 remained higher (88 μM), and it still
216 penetrated into the surface sediment down to 1.1 mm. In August, free S^{2-} was present near the
217 sediment-water interface at all three stations, and the concentration of S^{2-} in the porewater
218 increased with water depth.

219 Bottom water NH_4^+ concentration at S1 ranged from 3 μM in March to 11.5 μM in August;
220 NO_2^- concentration was relatively constant (0.7–1 μM) in March and August. NO_3^- concentration
221 ranged from 28 μM in March to < 2 μM in August in S1, whereas in S2 and S3 it varied between
222 28 μM in March and ca. 10 μM in August (Table 1; for detailed bottom water biogeochemistry
223 see Seitaj et al., 2015; Hagens et al., 2015; Sulu-Gambari et al., 2016; Lipsewers et al., 2016).
224 Sediment TOC content varied slightly between stations and seasons, ranging between 1.8 and 4.4
225 % as described previously (Table 1; Lipsewers et al., 2016).

226 *3.2. Archaeal 16S rRNA gene diversity and abundance*

227 Archaeal diversity was estimated from 16S rRNA gene amplicon sequencing using universal
228 primers. The archaeal community was dominated by Thaumarchaeota marine group I (MGI) in
229 March at both S1 and S3, with 72–82% of the total archaeal reads (Fig. 2(A), Table A.1). At S2
230 these Archaea were slightly less dominant but still comprised almost half of the total archaeal
231 reads. Other archaeal groups were also present in the surface sediment in March in addition to
232 MGI, such as members of the phylum *Candidatus* Woesearchaeota within the DPANN (referred
233 here as DPANN Woesearchaeota; DHVE-6; 16–31%), Thermoplasmatales (3–14%) and MCG
234 (1.4–2.5%). In August, the proportion of reads attributed to the DPANN Woesearchaeota
235 increased notably from 16 to 95% at S1, from 31 to 66% at S2 and from 21 to 57% at S3, at the
236 expense of the reads assigned to the Thaumarchaeota MGI (Fig. 2(A), Table A.1). In addition, a
237 slight increase in the proportion of reads was observed from March to August for Archaea
238 affiliated to the MCG and Thermoplasmatales groups. Total archaeal abundance estimated from
239 qPCR with general Archaea 16S rRNA gene primers was comparable between March and August
240 in all stations, with slightly lower values at S1 (avg. 6×10^9 gene copies/g) and $1–2 \times 10^{10}$ gene
241 copies/g for S2 and S3 (Fig. 2(B)).
242 The diversity of Thaumarchaeota was further analyzed by way of amplification, cloning and
243 sequencing of the *amoA* gene in the surface sediments of the three stations. All *amoA* sequences
244 were closely related to sequences previously detected in marine surface sediments. Although
245 certain variability was detected between the sequences recovered from different stations and
246 seasons, no clear clustering was observed (Fig. 3).
247 *3.2. Archaeal lipid diversity and distribution*
248 The archaeal IPL-GDGT concentration (quantified as IPL-derived CLs) was almost an order
249 of magnitude higher in March at all stations in comparison with the values in August, although

the decrease was less for S3, where slightly lower concentrations of GDGT-0 and crenarchaeol were detected in March in comparison with the other stations (Table 2). In March, total IPL-GDGTs were distributed mainly between IPL-GDGT-0 (ca. 5 μg/g dry wt sediment) and IPL-crenarchaeol (avg. 2.6 μg/g). In August, the total IPL-GDGT abundance was lower in comparison with March (ca. an order of magnitude less), while the distribution did not change (Table 2). CL-GDGT abundance was also higher in March (26 to 79 μg/g) than in August (5 to 15 μg/g; Table 2). CL-GDGT abundance was also higher than those of IPL-GDGTs at all stations and seasons (Table 2). At S1 it was on average 3x higher in both March and August. On the other hand, at S2, CL-GDGTs were on average 8x higher than IPL-GDGTs in March and 30x higher in August, with CL-crenarchaeol the most abundant CL-GDGT in August (8 μg/g; Table 2), 40x more than IPL-crenarchaeol (0.2 μg/g; Table 2). At S3, CL-GDGTs were on average 4x higher in concentration than IPL-GDGTs (Table 2).

The IPL composition was assessed from UHPLC-HRMS analysis and various IPL-GDGTs and IPL-archaeol were specifically targeted by using an inclusion list as part of the analytical routine (see supplementary File A.1). Within the various IPL types, the distribution for the cores was comparable to the distribution obtained after analysis of the IPL-derived CLs. IPLs with GDGT-0 and crenarchaeol as CL were the most abundant IPLs, with the highest concentrations in March (ca. 10^{10} response units/g), while IPLs with GDGT-1 and -2 as CLs were two orders of magnitude less abundant (Table 3). In August, total IPL-GDGT concentration decreased by two orders of magnitude vs. the concentration in March. In March, both IPLs with GDGT-0 and crenarchaeol cores were found with mainly HPH as IPL type, while in August the IPL type MH increased at the expense of HPH (Table 3) as also observed in the distribution of the relative

abundance of the different lipids (Table A.2). IPL-archaeol was only found at S1 in March with DH as a headgroup (Table 3).

4. Discussion

The seasonal changes in O_2 and S^{2-} concentration in the bottom water triggered an important switch in the archaeal community composition in the surface sediment. The archaeal community changed considerably from Thaumarchaeota MGI-dominated in March, when O_2 was still present and S^{2-} was absent (Table 1) to an archaeal community dominated by Archaea of the DPANN Woesearchaeota, although the seasonal change did not induce a diversity change within the Thaumarchaeota, as indicated by the *amoA* gene diversity (Fig. 3).

By multiplying the proportion of 16S rRNA gene reads for the Thaumarchaeota and the DPANN Woesearchaeota by the total Archaea 16S rRNA gene copies/g sediment, we could estimate the abundances of these groups (Table 4; assuming one 16S rRNA gene copy number per genome). For Thaumarchaeota, the abundance decreased dramatically at S1 (from 6×10^9 cells/g to undetected) and at S3 (2×10^{10} to 1.2×10^9 cells/g), while at S2 it remained fairly constant (Table 4). On the other hand, members of the DPANN Woesearchaeota were the major component of the archaeal population in August at all stations, with absolute numbers increasing (1×10^9 to 4.2×10^9 cells/g sediment at S1; 2×10^9 to 2×10^{10} cells/g at S2, 6.4×10^9 to 1.2×10^{10} cells/g at S3; Table 4). The change in the archaeal community is entirely compatible with the metabolism of both Thaumarchaeota and the DPANN Archaea, which is aerobic (Könneke *et al.*, 2005) and anaerobic (Castelle et al., 2015), respectively. Also, nitrification conducted by Thaumarchaeota has been shown to be inhibited by S^{2-} (Berg et al., 2015), which also explains the decrease in MGI population upon increase in S^{2-} concentration in the summer. In the same way, the abundance of the other archaeal benthic groups, which increased in the surface

sediments in August, such as the Thermoplasmatales and the MCG, are predicted to have an anaerobic metabolism based on their genome. The environmental control of the change in the archaeal community diversity is supported by the fact that this change is less evident in the surface sediment of S3, where O_2 was still present and the S^{2-} concentration in summer was substantially lower than at S1 and S2 (Table 1). Although the seasonality changes in physicochemical conditions in the bottom water and porewater induced a large change in the archaeal community diversity, the total archaeal abundance remained fairly constant between seasons and at the different stations (Fig. 2(B)). The archaeal community analysis was conducted using primer-based 16S rRNA gene amplicon sequencing. Therefore, we cannot completely rule out a possible primer bias (Sipos et al., 2010; Schloss et al., 2011), although the under representation of DPANN sequences in the databases would imply that, if any of these primer biases were to negatively detect DPANN in our samples, this would induce an underestimation of this group.

The large change in the archaeal community composition in the surface sediments upon the decrease in O_2 in the summer coincided with an order of magnitude decrease in the total IPL-GDGTs, which is connected to the decrease of the Thaumarchaeota population reported by the quantitative PCR and sequencing data. The IPL-GDGT profiles in March were compatible with a Thaumarchaeota-dominated population, due to the relatively high abundance of crenarchaeol, the specific CL of Thaumarchaeota (Sinninghe Damsté et al., 2002). In addition, the IPLMH-crenarchaeol (and all other main GDGTs) increased at the expense of the HPH-IPL from March to August (Table 3). The predominance of HPH IPL-crenarchaeol has been interpreted as an indication of the presence of an active Thaumarchaeotal population synthesizing membrane lipids in situ (Lengger et al., 2012, 2014), due to the labile nature of HPH IPLs (Harvey et al., 1986; Schouten et al., 2010). On the other hand, glycolipid-type IPLs (here mainly MH) have been

considered as a fossil signal (Lengger et al., 2012, 2014) or, alternatively, as the preferred IPL type in conditions where the Thaumarchaeota are in a stationary phase of growth (Elling et al., 2014). Therefore, the presence of glycolipid-IPLs in the surface sediments in August could be interpreted as a remnant of a Thaumarchaeota population previously existing in March, as supported by the sequencing data, or alternatively a population of Thaumarchaeota that are in stationary phase of growth due to the unfavorable (hypoxic and sulfidic) conditions.

Recent studies suggest that members of the DPANN have a reduced genome with limited metabolic capability (Rinke et al., 2013; Castelle et al., 2015), suggesting that these Archaea may have a symbiotic or parasitic lifestyle. In addition, most of the DPANN Archaea genomes available also lack most if not all the genes coding for the enzymes of the archaeal lipid biosynthetic pathway with the exception of the genomes of the phylum Candidatus Micrarchaeota and the genome of *Ca.* Iainarchaeum andersonii which harbor homologs of the geranylgeranylglyceryl phosphate (GGGP) and the digeranylgeranylglyceryl phosphate (DGGGP) synthase mediating the formation of the two ether bond between the isoprenoid side chains and the glycerol-1-phosphate as overview in Table A.3 (Jahn et al., 2004; Villanueva et al., 2017). They are therefore not expected to contribute to the total IPL-GDGT pool by actively synthesizing lipids but may recycle the membrane lipids of other Archaea. The decline in the total archaeal IPL-GDGTs in August coinciding with the switch to a DPANN Woesearchaeota-dominant population with similar or even higher cell abundance to that in March would therefore imply that the DPANN Woesearchaeota make use of the preserved ('fossil') pool of IPL-GDGTs to make their membranes. Alternatively, this DPANN Woesearchaeota population could potentially be using another archaeal membrane lipid not detected in our analysis. Apart from IPL-GDGTs, IPL-archaeol with dihexose polar head group was detected only in the surface

sediment of S1 in March (Table 3), therefore it seems unlikely that archaeol could be the archaeal membrane lipid source of the DPANN Woesearchaeota.

A question remains with respect to the potential membrane lipid acquisition mechanism regarding if the pool of 'fossil' IPL-GDGTs would be able to fulfill the membrane requirements of the large archaeal DPANN population detected in the surface sediments sampled in August in view of the much reduced concentration of IPL-GDGTs, which is an order of magnitude lower. This can only work when the DPANN Archaea have a much smaller cell size than the Thaumarchaeota that thrive in spring. The size of the DPANN Woesearchaeota in Lake Grevelingen surface sediment is unknown. The only characterized archaeon from the DPANN super phylum is *Nanoarchaeum equitans,* which is considered to be a symbiont of the archaeon *Ignicoccus* sp. by growing on its surface. The lipids of *N. equitans* have been shown to be derived from *Ignicoccus* sp. (Jahn et al., 2004), but the uptake mechanism is unknown. *N. equitans* is 5x smaller than its host, the archaeon *Ignicoccus* sp. Assuming a similar size difference between the DPANN Woesearchaeota in Lake Grevelingen surface sediments and its potential host, sufficient IPLs would be available to sustain the DPANN population detected in the sediments in August.

Alternatively, the DPANN Archaea could recycle the CL-GDGTs present in the sediment, as suggested by Takano et al. (2010) and Liu et al. (2011), which is presumed to involve hydrolysis and reformation of the ether bond to the glycerol backbone, as suggested by the ^{13}C-glucose labeling studies of Takano et al. (2010). However, since the members of the DPANN generally lack the gene coding for the enzymes involved in producing the ether bonds to the glycerol backbone (Villanueva *e*t al., 2017), this is unlikely. Alternatively, they could also use the CL-GDGTs and add the polar head groups de novo. Waters et al. (2003) observed the presence of genes for lipid modification, such as glycosylation, in the genome of *N. equitans*. We performed a search for the gene encoding cytidine diphosphate (CDP)-archaeol synthase (CarS, E.C.

2.7.7.67) that catalyzes the activation of 2,3-bis-*O*-geranylgeranylglyceryl diphosphate (DGGGP) by cytidine triphosphate (CTP) to form the intermediate for polar head group attachment (i.e. CDP-archaeol), and we found homologs in most of the DPANN Micrarchaeota genomes and in some of the DPANN Parvarchaeota and Diapherotrites (Table A2; performed by way of find function in JGI Integrated Microbial Genomes, IMG with genomes available in November 2017). However, the genes coding for the enzymes that catalyze the subsequent replacement of cytidine monophosphate of the cytidine diphosphate (CDP)-archaeol of CDP-diacylglycerol with a polar head group in DPANN genomes were not detected, in contrast to *N. equitans* (Waters *et al*., 2003). This may indicate that the members of the DPANN either do not have the capacity of adding the polar head groups to the CL-GDGT or that the polar head groups of their IPLs are different and added by enzymes different from those already characterized.

5. Conclusions

We observed a dramatic change in the archaeal community composition and lipid abundance in surface sediments of a seasonally hypoxic marine lake, which corresponded to a switch from a Thaumarchaeota-dominated to a DPANN-dominated archaeal community, while the total IPLs were significantly reduced. Considering the reduced genome of the members of the super phylum DPANN and their apparent inability to synthesize their own membrane lipids, we hypothesize that they use the CLs previously synthesized by the Thaumarchaeota to form their membrane.

Acknowledgements

We acknowledge the crew of the R/V Luctor and P. van Rijswijk for help in the field during sediment collection, M. van der Meer and S. Heinzelmann for support onboard and assistance

with incubations, E. Panoto for technical support, and E. Boschker and F. Meysman for helpful discussions. The work was financially supported by the Darwin Centre for Biogeosciences to L.V. (grant no. 3062). L.V. and J.S.S.D receive funding from the Soehngen Institute for Anaerobic Microbiology (SIAM) through a Gravitation Grant (024.002.002) from the Dutch Ministry of Education, Culture and Science (OCW).

References

Altschul, S.F., Gish, W., Miller, W., Myers, E.W., Lipman, D.J., 1990. Basic local alignment search tool. Molecular Biology 215, 403–410.

Bauersachs, T., Speelman, E.N., Hopmans, E.C., Reichart, G.-J., Schouten, S., Sinninghe Damsté, J.S., 2010. Fossilized glycolipids reveal past oceanic N_2 fixation by heterocystous cyanobacteria. Proceedings of the National Academy of Sciences107, 1–5.

Berg, C., Vandieken, V., Thamdrup, B., Jürgens, K., 2015. Significance of archaeal nitrification in hypoxic waters of the Baltic Sea. The ISME Journal 9, 1319–1332.

Biddle, J.F., Lipp, J.S., Lever, M.A., Lloyd, K.G., Sørensen, K.B., Anderson, R., Fredricks, H.F., Elvert, M., Kelly, T.J., Schrag, D.P., Sogin, M.L., Brenchley, J.E., Teske, A., House, C.H., Hinrichs, K.-U., 2006. Heterotrophic Archaea dominate sedimentary subsurface ecosystems off Peru. Proceedings of the National Academy of Sciences 103, 3846–3851.

Bligh, E.G., Dyer, W.J., 1959. A rapid method of total lipid extraction and purification. Canadian Journal of Biochemistry and Physiology 37, 911–917.

Castelle, C.J., Wrighton, K.C., Thomas, B.C., Hug, L.A., Brown, C.T., Wilkins, M.J., Frischkorn, K.R., Tringe, S.G., Singh, A., Markillie, L.M., Taylor, R.C., Williams, K.H., Banfield, J.F., 2015. Genomic expansion of domain Archaea highlights roles for organisms from new phyla in anaerobic carbon cycling. Current Biology 25, 690–701.

Comolli, L.R., Baker, B.J., Downing, K.H., Siegerist, C.E., Banfield, J.F., 2009. Three-dimensional analysis of the structure and ecology of a novel, ultra-small archaeon. The ISME Journal 3, 159–167.

Edgar, R.C., 2004. MUSCLE: Multiple sequence alignment with high accuracy and high throughput. Nucleic Acids Research 32, 1792–1797.

Elling, F.J., Könneke, M., Lipp, J.S., Becker, K.W., Gagen, E.J., Hinrichs, K.-U., 2014. Effects of growth phase on the membrane lipid composition of the thaumarchaeon *Nitrosopumilus maritimus* and their implications for archaeal lipid distributions in the marine environment. Geochimica et Cosmochimica Acta. 141, 579–597.

Hagens, M., Slomp, C.P., Meysman, F.J.R., Seitaj, D., Harlay, J., Borges, A.V., Middelburg, J.J., 2015. Biogeochemical processes and buffering capacity concurrently affect acidification in a seasonally hypoxic coastal marine basin. Biogeosciences 12, 1561–1583.

Harvey, H.R., Fallon, R.D., Patton, J.S., 1986. The effect of organic matter and oxygen on the degradation of bacterial membrane lipids in marine sediments. Geochimica et Cosmochimica Acta 50, 795–804.

Huguet, C., Cartes, J.E., Sinninghe Damsté, J.S., Schouten, S., 2006a. Marine crenarchaeotal membrane lipids in decapods: Implications for the TEX_{86} paleothermometer. Geochemistry, Geophysics, Geosystems 7, Q11010.

Huguet, C., Hopmans, E.C., Febo-Ayala, W., Thompson, D.H., Sinninghe Damsté, J.S., Schouten, S., 2006b. An improved method to determine the absolute abundance of glycerol dibiphytanyl glycerol tetraether lipids. Organic Geochemistry 37, 1036–1041.

Jahn, U., Summons, R., Sturt, H., Grosjean, E., Huber, H., 2004. Composition of the lipids of *Nanoarchaeum equitans* and their origin from its host *Ignicoccus* sp. strain KIN4/I. Archives of Microbiology 182, 404–413.

Jarrell, K.F., Walters, A.D., Bochiwal, C., Borgia, J.M., Dickinson, T., Chong, J.P.J., 2011. Major players on the microbial stage: Why Archaea are important. Microbiology 157, 919–936.

Kim, J.H., van der Meer, J., Schouten, S., Helmke, P., Willmott, V., Sangiorgi, F., Koç, N., Hopmans, E.C., Sinninghe Damsté, J.S., 2010. New indices and calibrations derived from the distribution of crenarchaeal isoprenoid tetraether lipids: Implications for past sea surface temperature reconstructions. Geochimica et Cosmochimica Acta 74, 4639–4654.

Klindworth, A., Pruesse, E., Schweer, T., Peplies, J., Quast, C., Horn, M., Glöckner, F.O., 2013. Evaluation of general 16S ribosomal RNA gene PCR primers for classical and next-generation sequencing-based diversity studies. Nucleic Acids Research 41, 1–11.

Könneke, M., Bernhard, A.E., de la Torre, J.R., Walker, C.B., Waterbury, J.B., Stahl, D.A., 2005. Isolation of an autotrophic ammonia-oxidizing marine archaeon. Nature 437, 543–546.

Kubo, K., Lloyd, K.G., F Biddle, J., Amann, R., Teske, A., Knittel, K., 2012. Archaea of the Miscellaneous Crenarchaeotal Group are abundant, diverse and widespread in marine sediments. The ISME Journal 6, 1949–1965.

Lengger, S.K., Hopmans, E.C., Sinninghe Damsté, J.S., Schouten, S., 2012. Comparison of extraction and work up techniques for analysis of core and intact polar tetraether lipids from sedimentary environments. Organic Geochemistry 47, 34–40.

Lengger, S.K., Lipsewers, Y.A., Haas, H. De, Sinninghe Damsté, J.S., Schouten, S., 2014. Lack of ^{13}C-label incorporation suggests low turnover rates of thaumarchaeal intact polar tetraether lipids in sediments from the Iceland shelf. Biogeosciences 11, 201–216.

Lipp, J.S., Hinrichs, K.-U., 2009. Structural diversity and fate of intact polar lipids in marine sediments. Geochimica et Cosmochimica Acta 73, 6816–6833.

Lipp, J.S., Morono, Y., Inagaki, F., Hinrichs, K.-U., 2008. Significant contribution of Archaea to extant biomass in marine subsurface sediments. Nature 454, 991–994.

Lipsewers, Y.A., Hopmans, E.C., Meysman, F.J.R., Sinninghe Damsté, J.S., Villanueva, L., 2016. Abundance and diversity of denitrifying and anammox bacteria in seasonally hypoxic and sulfidic sediments of the saline Lake Grevelingen. Frontiers in Microbiology 7, 1–15.

Lipsewers, Y.A., Vasquez-Cardenas, D., Seitaj, D., Schauer, R., Hidalgo-Martinez, S., Sinninghe Damsté, J.S., Meysman, F.J.R., Villanueva, L., Boschker, H.T.S., 2017. Impact of seasonal hypoxia on activity and community structure of chemolithoautotrophic bacteria in a coastal sediment. Applied and Environmental Microbiology 83, e03517–16.

Liu, X., Lipp, J.S., Hinrichs, K.-U., 2011. Distribution of intact and core GDGTs in marine sediments. Organic Geochemistry 42, 368–375.

Lloyd, K.G., May, M.K., Kevorkian, R.T., Steen, D., 2013. Meta-analysis of quantification methods shows that Archaea and Bacteria have similar abundances in the subseafloor. Applied and Environmental Microbiology 79, 7790–7799.

Logemann, J., Graue, J., Köster, J., Engelen, B., Rullkötter, J.,, Cypionka, H. 2010. A laboratory experiment of intact polar lipid degradation in sandy sediments. Biogeosciences 8, 2547–2560.

Ma, Y., Liu, F., Kong, Z., Yin, J., Kou, W., Wu, L., Ge, G., 2016. The distribution pattern of sediment archaea community of the Poyang Lake, the largest freshwater lake in China. Archaea. Volume 2016, Article ID 9278929, 12 pages http://dx.doi.org/10.1155/2016/9278929

Malkin, S.Y., Rao, A.M.F., Seitaj, D., Vasquez-Cardenas, D., Zetsche, E.-M., Hidalgo-Martinez, S., Boschker, H.T.S., Meysman, F.J.R., 2014. Natural occurrence of microbial sulfur oxidation by long-range electron transport in the seafloor. The ISME Journal 8, 1843–1854.

Meng, J., Xu, J., Qin, D., He, Y., Xiao, X., Wang, F., 2014. Genetic and functional properties of uncultivated MCG archaea assessed by metagenome and gene expression analyses. The ISME Journal 8, 650–659.

Moore, E.K., Villanueva, L., Hopmans, E.C., Rijpstra, W.I.C., 2015. Abundant trimethyl ornithine lipids and specific gene sequences indicate Planctomycete importance at the oxic/anoxic interface in Sphagnum -dominated northern wetlands. Applied and Environmental Microbiology 81, 6333– 6344.

Ortiz-Alvarez, R., Casamayor, E.O., 2016. High occurrence of Pacearchaeota and Woesearchaeota (Archaea superphylum DPANN) in the surface waters of oligotrophic high-altitude lakes. Environmental Microbiology Reports 8, 210–217.

Pearson, A., Huang, Z., Ingalls, A.E., Romanek, C.S., Wiegel, J., Freeman, K.H., Smittenberg, R.H., Zhang, C.L., 2004. Nonmarine crenarchaeol in Nevada hot springs. Applied and Environmental Microbiology 70, 5229–5237.

Pester, M., Schleper, C., Wagner, M., 2011. The Thaumarchaeota: an emerging view of their phylogeny and ecophysiology. Current Opinion in Microbiology 14, 300–306.

Pitcher, A., Hopmans, E.C., Mosier, A.C., Park, S.-J., Rhee, S.-K., Francis, C.A., Schouten, S., Sinninghe Damsté, J.S., 2011a. Core and intact polar glycerol dibiphytanyl glycerol tetraether lipids of ammonia-oxidizing archaea enriched from marine and estuarine sediments. Applied and Environmental Microbiology 77, 3468–3477.

Pitcher, A., Villanueva, L., Hopmans, E.C., Schouten, S., Reichart, G.-J., Sinninghe Damsté, J.S., 2011b. Niche segregation of ammonia-oxidizing archaea and anammox bacteria in the Arabian Sea oxygen minimum zone. The ISME journal 5, 1896–1904.

Quast, C., Pruesse, E., Yilmaz, P., Gerken, J., Schweer, T., Yarza, P., Peplies, J., Glöckner, F.O., 2013. The SILVA ribosomal RNA gene database project: improved data processing and web-based tools. Nucleic Acids Research 41, D590–596.

Rinke, C., Schwientek, P., Sczyrba, A., Ivanova, N.N., Anderson, I.J., Cheng, J.-F., Darling, A., Malfatti, S., Swan, B.K., Gies, E.A., Dodsworth, J.A., Hedlund, B.P., Tsiamis, G., Sievert, S.M., Liu, W.-T., Eisen, J. A., Hallam, S.J., Kyrpides, N.C., Stepanauskas, R., Rubin, E.M., Hugenholtz, P., Woyke, T., 2013. Insights into the phylogeny and coding potential of microbial dark matter. Nature 499, 431–437.

Saitou, N., Nei, M., 1987. The neighbor-joining method: a new method for reconstructing phylogenetic trees. Molecular Biology and Evolution 4, 406–425.

Schloss, P.D., Gevers, D., Westcott, S.L., 2011. Reducing the effects of PCR amplification and sequencing Artifacts on 16s rRNA-based studies. PLoS ONE 6, e27310.

Schouten, S., Hopmans, E.C., Schefuß, E., Sinninghe Damsté, J.S., 2002. Distributional variations in marine crenarchaeotal membrane lipids: A new tool for reconstructing ancient sea water temperatures? Earth and Planetary Science Letters 204, 265–274.

Schouten, S., Hopmans, E.C., Sinninghe Damsté, J.S., 2013. The organic geochemistry of glycerol dialkyl glycerol tetraether lipids: A review. Organic Geochemistry 54, 19–61.

Schouten, S., Middelburg, J.J., Hopmans, E.C., Sinninghe Damsté, J.S., 2010. Fossilization and degradation of intact polar lipids in deep subsurface sediments: A theoretical approach. Geochimica et Cosmochimica Acta 74, 3806–3814.

Seitaj, D., Schauer, R., Sulu-Gambari, F., Hidalgo-Martinez, S., Malkin, S.Y., Burdorf, L.D.W., Slomp, C.P., Meysman, F.J.R., 2015. Cable bacteria in the sediments of seasonally-hypoxic basins: a microbial "firewall" against euxinia. Proceedings of the National Academy of Sciences 112, 13278–13283.

529 Shah, S.R., Mollenhauer, G., Ohkouchi, N., Eglinton, T.I., Pearson, A., 2008. Origins of archaeal
530 tetraether lipids in sediments: Insights from radiocarbon analysis. Geochimica et
531 Cosmochimica Acta 72, 4577–4594.

532 Sinninghe Damsté, J.S., Rijpstra, W.I.C., Hopmans, E.C., Jung, M.Y., Kim, J.G., Rhee, S.K.,
533 Stieglmeier, M., Schleper, C., 2012. Intact polar and core glycerol dibiphytanyl glycerol
534 tetraether lipids of group I.1a and I.1b Thaumarchaeota in soil. Applied and Environmental
535 Microbiology 78, 6866–6874.

536 Sinninghe Damsté, J.S., Schouten, S., Hopmans, E.C., van Duin, A.C.T., Geenevasen, J.A.G.,
537 2002. Crenarchaeol: the characteristic core glycerol dibiphytanyl glycerol tetraether
538 membrane lipid of cosmopolitan pelagic crenarchaeota. The Journal of Lipid Research 43,
539 1641–1651.

540 Sipos, R., Székely, A., Révész, S., Márialigeti, K., 2010. Addressing PCR biases in
541 environmental microbiology studies. In: Cummings, S.P. (Ed.), Bioremediation Methods
542 and Protocols, Series Methods in Molecular Biology, 599. Humana press, pp. 37–58.

543 Sulu-Gambari, F., Seitaj, D., Meysman, F.J.R., Schauer, R., Polerecky, L., Slomp, C.P., 2016.
544 Cable bacteria control iron-phosphorus dynamics in sediments of a coastal hypoxic basin.
545 Environmental Science and Technology 50, 1227–1233.

546 Takano, Y., Chikaraishi, Y., Ogawa, N.O., Nomaki, H., Morono, Y., Inagaki, F., Kitazato, H.,
547 Hinrichs, K.-U., Ohkouchi, N., 2010. Sedimentary membrane lipids recycled by deep-sea
548 benthic archaea. Nature Geoscience 3, 858–861.

549 Villanueva, L., Schouten, S., Sinninghe Damsté, J.S., 2017. Phylogenomic analysis of lipid
550 biosynthetic genes of Archaea shed light on the "lipid divide." Environmental Microbiology
551 19, 54–69.

552 Wakeham, S.G., Lewis, C.M., Hopmans, E.C., Schouten, S., Sinninghe Damsté, J.S., 2003.
553 Archaea mediate anaerobic oxidation of methane in deep euxinic waters of the Black Sea.
554 Geochimica et Cosmochimica Acta 67, 1359–1374.

555 Waters, E., Hohn, M.J., Ahel, I., Graham, D.E., Adams, M.D., Barnstead, M., Beeson, K.Y.,
556 Bibbs, L., Bolanos, R., Keller, M., Kretz, K., Lin, X., Mathur, E., Ni, J., Podar, M.,
557 Richardson, T., Sutton, G.G., Simon, M., Soll, D., Stetter, K.O., Short, J.M., Noordewier,
558 M., 2003. The genome of *Nanoarchaeum equitans*: Insights into early archaeal evolution
559 and derived parasitism. Proceedings of the National Academy of Sciences 100, 12984–
560 12988.

561 White, D.C., Davis, W.M., Nickels, J.S., King, J.D., Bobbie, R.J., 1979. Determination of the
562 sedimentary microbial biomass by extractable lipid phosphate. Oecologica 62, 51–62.

Wuchter, C., Schouten, S., Coolen, M.J.L., Sinninghe Damsté, J.S., 2004. Temperature-dependent variation in the distribution of tetraether membrane lipids of marine Crenarchaeota: Implications for TEX_{86} paleothermometry. Paleoceanography 19, PA4028.

Wuchter, C., Schouten, S., Wakeham, S.G., Sinninghe Damsté, J.S., 2005. Temporal and spatial variation in tetraether membrane lipids of marine Crenarchaeota in particulate organic matter: Implications for TEX_{86} paleothermometry. Paleoceanography 20, PA3013.

Wuchter, C., Schouten, S., Wakeham, S.G., Sinninghe Damsté, J.S., 2006. Archaeal tetraether membrane lipid fluxes in the northeastern Pacific and the Arabian Sea: Implications for TEX_{86} paleothermometry. Paleoceanography 21, PA4208.

Xie, S., Lipp, J.S., Wegener, G., Ferdelman, T.G., Hinrichs, K.U. 2013. Turnover of microbial lipids in the deep biosphere and growth of benthic archaeal populations. Proceedings of the National Academy of Sciences USA 110, 6010–6014.

Zhang, C.L., Pearson, A., Li, Y.L., Mills, G., Wiegel, J., 2006. Thermophilic temperature optimum for crenarchaeol synthesis and its implication for archaeal evolution. Applied and Environmental Microbiology 72, 4419–4422.

Figure Legends

Fig. 1. Sampling locations in Lake Grevelingen.

Fig. 2. Phylogenetic tree of *amoA* protein sequences recovered from the surface sediment (0–1 cm) of S1-S3 in Lake Grevelingen during March and August constructed with the Neighbor-Joining method (Saitou and Nei, 1987). Scale bar indicates 2% sequence dissimilarity. Evolutionary distances were computed using the Poisson correction method with a bootstrap test of 1,000 replicates (values > 50% are shown on the branches).

Fig. 2. (A) Proportion (%) of total archaeal 16S rRNA gene reads and (B) archaeal 16S rRNA gene abundance (copy number/g sediment) in surface sediment (0–1cm) of S1-S3 in March and in August. Only archaeal groups > 3% are reported; qPCR conditions, efficiency 90%; R^2 0.991.

Figure 1

Click here to download high resolution image

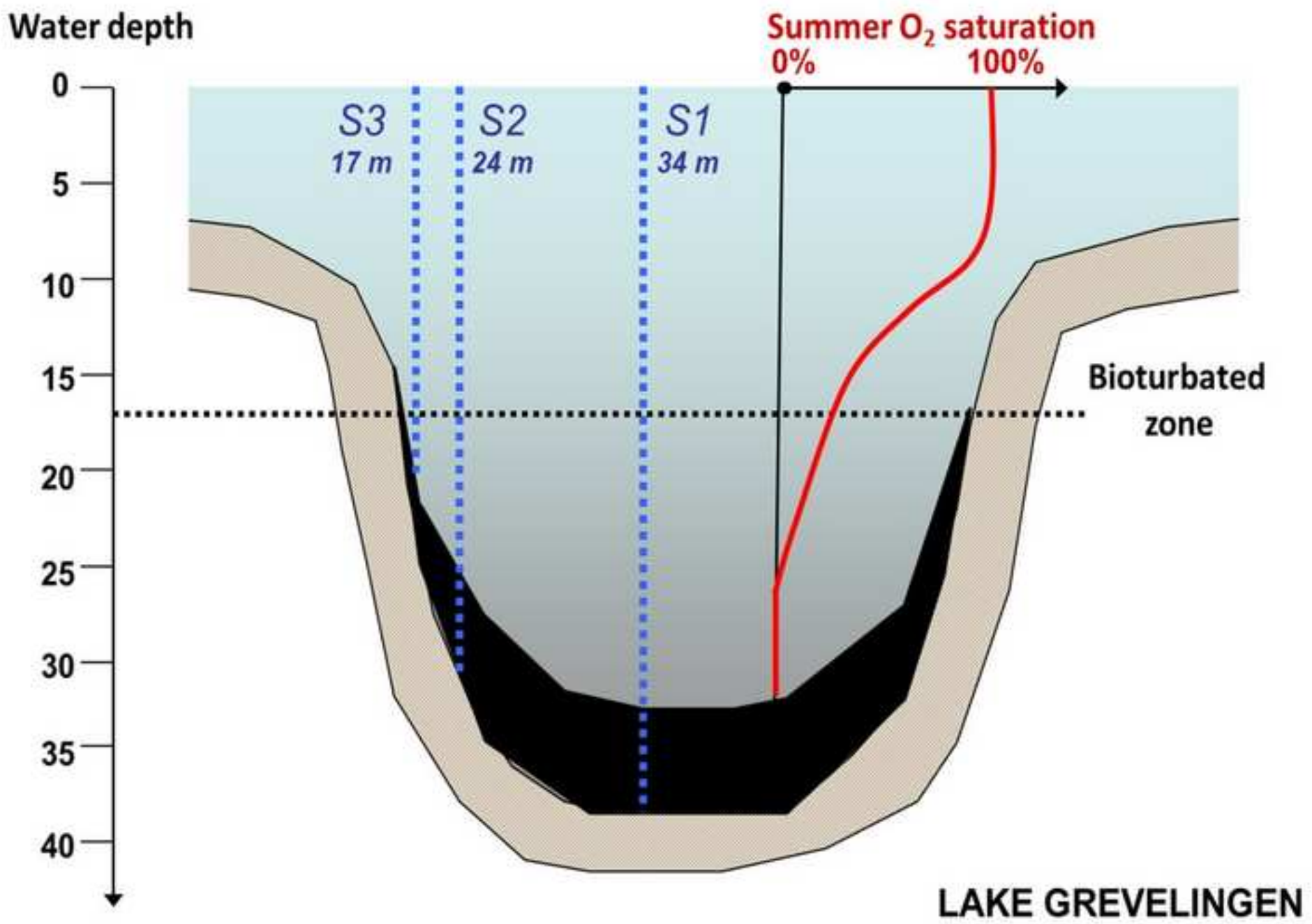

Figure 2A

Click here to download high resolution image

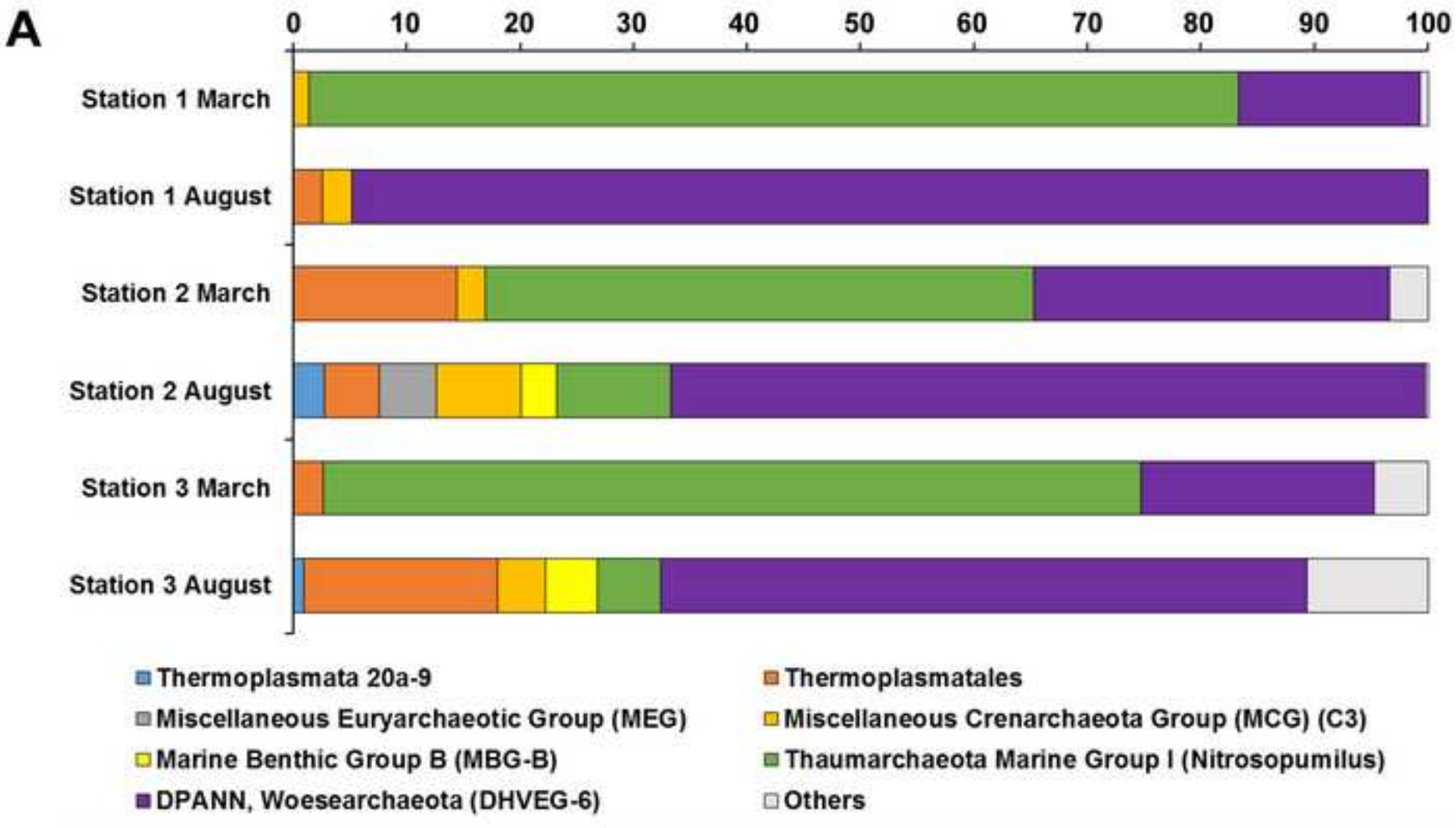

Figure 2B

Click here to download high resolution image

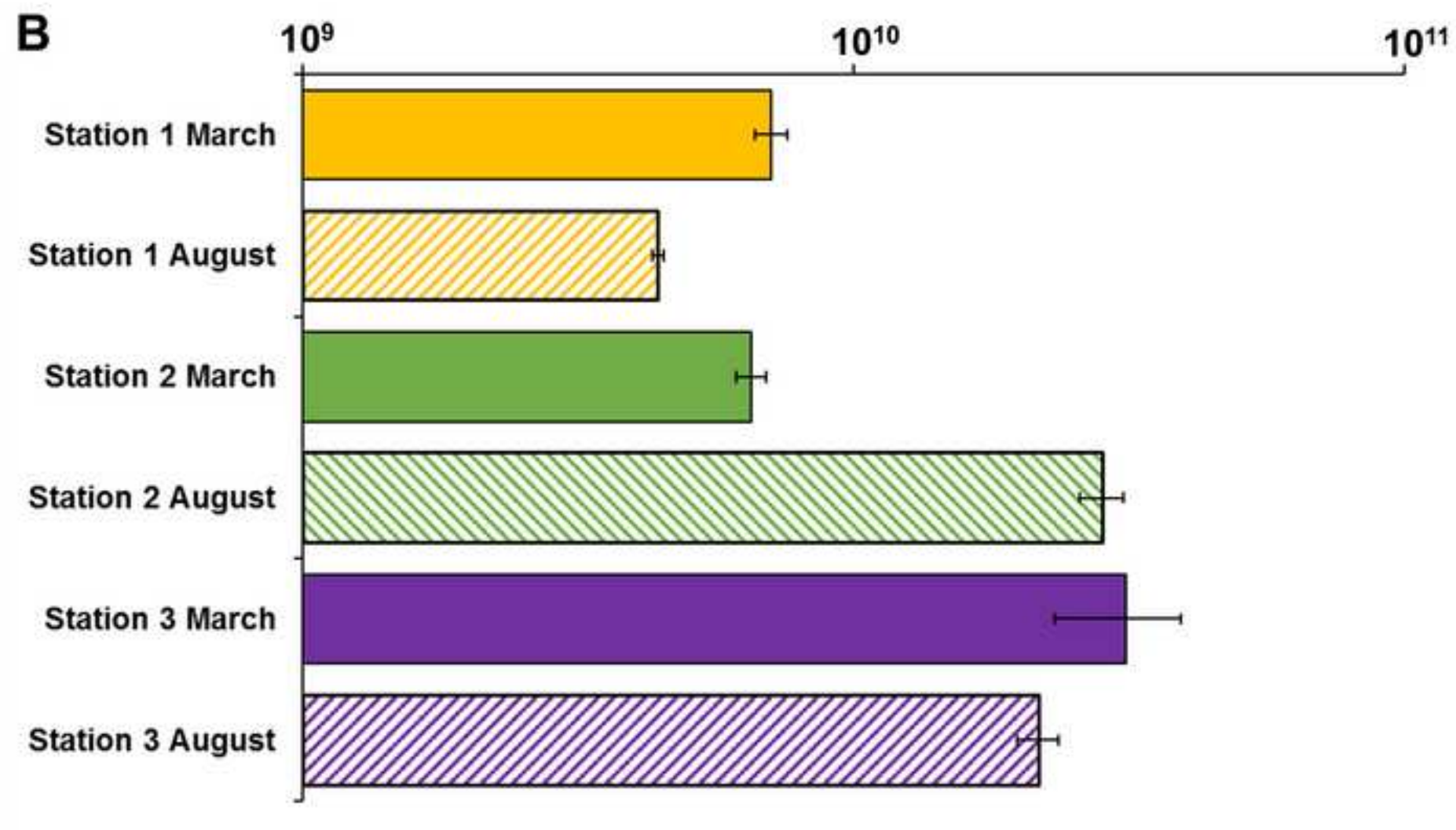

Figure 3

Click here to download high resolution image

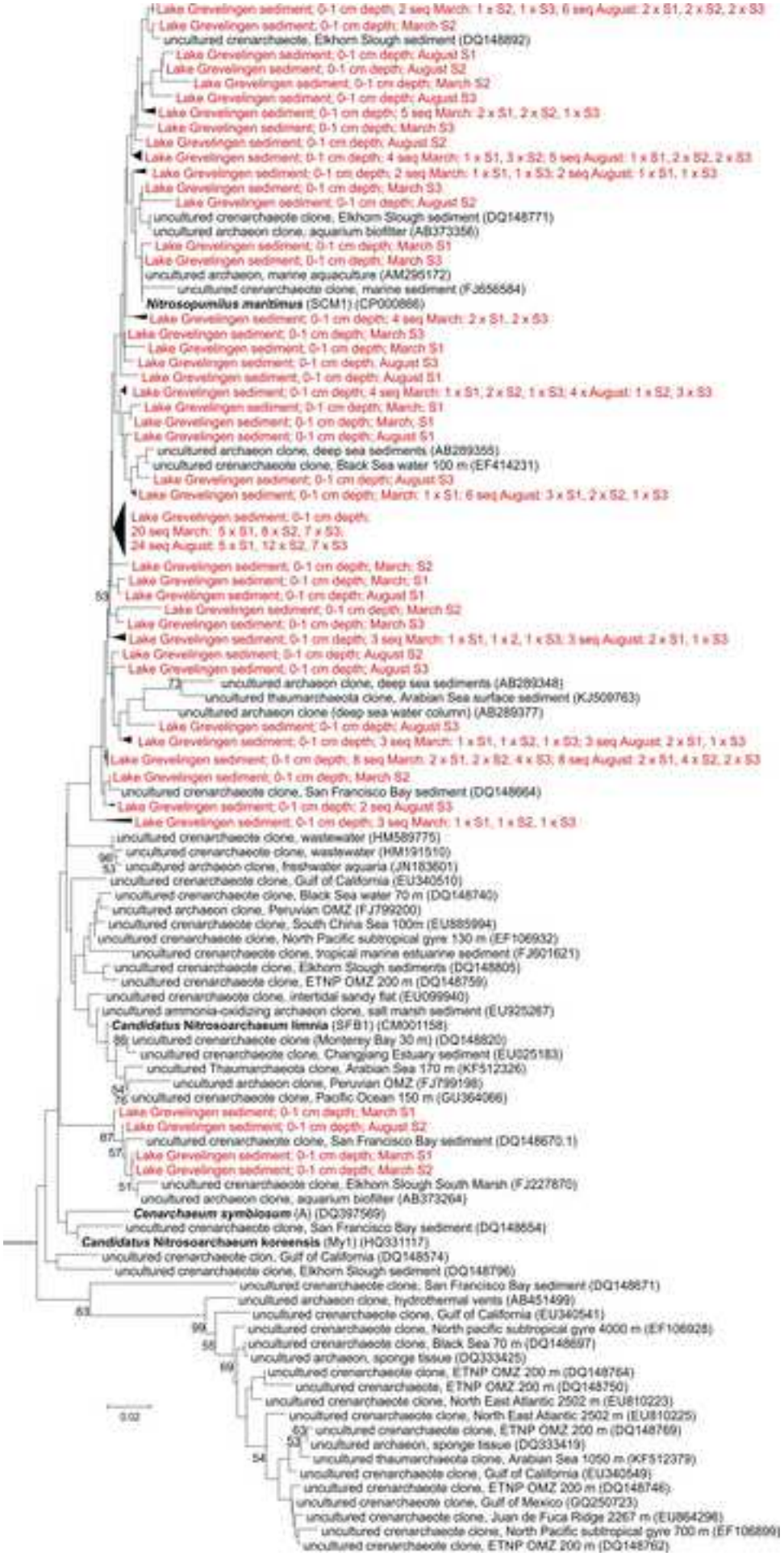

Table 1

Physicochemical parameters for bottom water and surface sediment (0–1 cm) at the three stations (S1-S3) in Lake Grevelingen in spring (March) and summer (August; data included in Seitaj et al., 2015; Sulu-Gambari et al., 2016; Hagens et al., 2015; Lipsewers et al., 2016).

	S1		S2		S3	
	March	August	March	August	March	August
Bottom water[a]						
(°C)	5	17	5	17	5	19
O_2 [μM]	299 (oxic)	0 (anoxic)	301 (oxic)	12 (hypoxic)	307 (oxic)	88 (hypoxic)
NH_4^+ [μM]	3.2	11.5	3.0	4.3	2.8	2.5
NO_2^- [μM]	0.7	1.0	0.7	0.7	0.7	0.1
NO_3^- [μM]	28.2	1.7	27.9	11.6	27.7	10.6
Surface sediment						
HS^- [μM]	0	810	0	1157	0	211
NH_4^+ [μM]	279	656	165	550	73	537
TOC (%)	2.86	1.81	3.11	2.38	2.87	3.04
OPD (mm)[b]	1.8±0.04	0	2.6±0.65	0	2.4±0.4	1.1±0.1
SAD (mm)[c]	17.5±0.7	0.9±1.1	21.3±2.5	0.6±0	41.8±8.6	4.2±2.7

[a] Classified as anoxic with O_2 < 1 μM and hypoxic < 63 μM; [b] O_2 penetration depth; [c] $\sum H_2S$ appearance depth.

Table 2

Abundance and distribution[a] of IPL-derived (released by acid hydrolysis) and CL-GDGTs (µg/g dry wt) in the surface sediment (0–1 cm) of the three stations (S1-S3) in Lake Grevelingen in spring (March) and summer (August).

	S1		S2		S3	
	March	August	March	August	March	August
IPL-derived GDGTs						
GDGT-0	5.1 (56.9)	0.8 (48.2)	5.9 (60.5)	0.2 (45.5)	3.0 (58.6)	1.7 (54.6)
GDGT-1	0.4 (4.6)	0.1 (5.5)	0.4 (4.4)	0.02 (4.9)	0.3 (5)	0.1 (4.6)
GDGT-2	0.2 (2.2)	0.1 (3.7)	0.2 (2.2)	0.01 (2.6)	0.1 (2.7)	0.1 (2.3)
GDGT-3	0.1 (0.9)	0.02 (1.3)	0.1 (0.8)	0.01 (1.1)	0.05 (1)	0.03 (0.9)
Cren[b]	3.1 (34.8)	0.6 (40.8)	3.1 (31.6)	0.2 (44.8)	1.7 (32.5)	1.1 (37.2)
Cren[c]	0.04 (0.5)	0.01 (0.5)	0.04 (0.4)	0.01 (1.1)	0.02 (0.3)	0.01 (0.4)
TOTAL	9.0	1.6	9.7	0.5	5.1	3.0
CL-GDGTs						
GDGT-0	12.9 (44)	2.1 (43)	36.2 (46)	5.8 (39.3)	11.8 (45.3)	2.9 (40.8)
GDGT-1	1.1 (3.7)	0.2 (3.6)	2.9 (3.7)	0.5 (3.5)	0.9 (3.5)	0.2 (3.5)
GDGT-2	0.5 (1.6)	0.1 (1.6)	1.3 (1.6)	0.2 (1.4)	0.4 (1.5)	0.1 (1.5)
GDGT-3	0.2 (0.8)	0.04 (0.7)	0.6 (0.8)	0.1 (0.7)	0.2 (0.7)	0.05 (0.7)
Cren[b]	14.5 (49.5)	2.5 (50.5)	37.5 (47.6)	8.1 (54.8)	12.7 (48.8)	3.7 (53)
Cren'[c]	0.1 (0.4)	0.03 (0.5)	0.3 (0.4)	0.04 (0.3)	0.1 (0.2)	0.04 (0.6)
Total	29.2	4.9	78.8	14.8	26.0	7.1

[a]Values in parentheses correspond to fractional (relative) abundance of each individual GDGT as the concentration of the individual GDGT divided by the sum of the concentration of all GDGTs in that fraction; [b] crenarchaeol; [c] crenarchaeol regioisomer.

Table 3

Absolute abundance (response units, r.u/g dry weight of archaeal IPLs; n.d., not detected) in surface sediments (0–1cm).

Intact Polar lipids	S1		S2		S3	
	March	August	March	August	March	August
GDGT-0-MH	9.4×10^{7}	1.3×10^{7}	3.1×10^{8}	4.4×10^{7}	1×10^{8}	4.9×10^{7}
GDGT-0-DH	6.3×10^{7}	n.d.	7.3×10^{7}	n.d.	6.7×10^{7}	n.d.
GDGT-0-DH[b]	2×10^{8}	n.d.	2.1×10^{8}	n.d.	1.4×10^{8}	2.6×10^{7}
GDGT-0-HPH	1.7×10^{10}	3.3×10^{8}	1.9×10^{10}	8.5×10^{8}	1.4×10^{10}	1.8×10^{9}
GDGT-1-MH	9.4×10^{7}	n.d.	8.9×10^{6}	n.d.	1.2×10^{6}	n.d.
GDGT-1-DH	1.9×10^{8}	n.d.	2.1×10^{8}	n.d.	6.2×10^{7}	n.d.
GDGT-1-DH[b]	n.d.	n.d.	n.d.	n.d.	8.2×10^{7}	n.d.
GDGT-1-HPH	4.6×10^{8}	n.d.	3.4×10^{8}	n.d.	5.2×10^{8}	n.d.
GDGT-2-DH	1.4×10^{8}	n.d.	2.7×10^{8}	n.d.	1.1×10^{8}	n.d.
GDGT-3-DH	8×10^{6}	n.d.	2.7×10^{7}	n.d.	1×10^{7}	n.d.
GDGT-3-DH[b]	n.d.	n.d.	1.2×10^{7}	n.d.	n.d.	n.d.
GDGT-4-DH	7.8×10^{7}	n.d.	1.5×10^{8}	n.d.	5×10^{7}	n.d.
GDGT-4-DH[b]	n.d.	n.d.	n.d.	n.d.	1.3×10^{7}	n.d.
Crenarchaeol-MH	1.5×10^{8}	5.3×10^{7}	3.1×10^{8}	5.7×10^{7}	9.5×10^{7}	7×10^{7}
Crenarchaeol-HPH	1.1×10^{10}	2.4×10^{8}	8.5×10^{9}	6.1×10^{8}	6.6×10^{9}	1.5×10^{9}
Archaeol-DH	3.8×10^{8}	n.d.	n.d.	n.d.	n.d.	n.d.
Total ru/g	3.0×10^{10}	8.7×10^{8}	3.0×10^{10}	1.6×10^{9}	2.2×10^{10}	3.4×10^{9}

[a] MH, monohexose; DH, dihexose; HPH, hexose phosphohexose; [b] isomer.

Table 4

Archaeal class abundance (cells/g sediment) calculated by multiplying the proportion (%) of total archaeal 16S rRNA gene reads by the archaeal 16S rRNA gene abundance (copy number/ sediment) in surface sediment (0–1cm) of the three stations S1-S3 in March and August, assuming one 16S rRNA gene copy number per genome (n.d., not detected).

Organism	S1		S2		S3	
	March	August	March	August	March	August
Thermoplasmata, 20a-9	n.d	n.d	n.d	7.8×10^8	n.d	2.0×10^8
Thermoplasmatales, AMOS1A-4113-D04	n.d	n.d	5.5×10^7	6.0×10^7	4.1×10^8	6.0×10^8
Thermoplasmatales, CCA47	n.d	n.d	1.7×10^8	2.4×10^8	2.3×10^8	1.7×10^7
Thermoplasmatales, MBG-D[a] & DHVEG-1	n.d	1.1×10^8	6.1×10^8	7.8×10^8	1.2×10^8	2.0×10^8
Thermoplasmatales, VC2.1 Arc6	n.d	n.d	1.1×10^8	3.0×10^8	5.8×10^7	1.2×10^9
Sum of reads Thermoplasmatales	n.d	1.1×10^8	9.4×10^8	1.4×10^9	8.2×10^8	3.7×10^9
Miscellaneous crenarchaeota group, C3	9.9×10^7	1.1×10^8	1.7×10^8	2.1×10^9	n.d	9.0×10^8
Thaumarchaeota, marine group I, *Nitrosopumilus*	5.8×10^9	n.d	3.1×10^9	2.9×10^9	2.2×10^{10}	1.2×10^9
Miscellaneous euryarchaeotic group (MEG)	n.d	n.d	n.d	1.4×10^9	n.d	n.d
DPANN, Woesearchaeota DHVEG-6	1.1×10^9	4.2×10^9	2.0×10^9	1.9×10^{10}	6.4×10^9	1.2×10^{10}
MBG-B[b]	n.d	n.d	n.d	9.0×10^8	n.d	1.0×10^9
Others	4.9×10^7	n.d	2.2×10^8	6.0×10^7	1.5×10^9	2.3×10^9
Total archaeal abundance (cell/g)	7.1×10^9	4.4×10^9	6.5×10^9	2.8×10^{10}	3.1×10^{10}	2.1×10^{10}
Total CL-GDGTs and IPL-derived GDGT μg g^{-1}	38.2	6.5	88.5	15.3	31.1	10.1
Calculated femtogram GDGT/cell	1.3	7.5	3.0	9.8	1.4	2.9

[a] Marine Benthic Group D; [b]Marine Benthic Group B.